

Photon-Mediated Interactions Between Distant Artificial Atoms

Arjan F. van Loo,^{1*} Arkady Fedorov,^{1†} Kevin Lalumière,² Barry C. Sanders,³ Alexandre Blais,² Andreas Wallraff¹

Photon-mediated interactions between atoms are of fundamental importance in quantum optics, quantum simulations, and quantum information processing. The exchange of real and virtual photons between atoms gives rise to nontrivial interactions, the strength of which decreases rapidly with distance in three dimensions. Here, we use two superconducting qubits in an open one-dimensional transmission line to study much stronger photon-mediated interactions. Making use of the possibility to tune these qubits by more than a quarter of their transition frequency, we observe both coherent exchange interactions at an effective separation of $3\lambda/4$ and the creation of super- and subradiant states at a separation of one photon wavelength λ . In this system, collective atom-photon interactions and applications in quantum communication may be explored.

In free space, the interaction of individual atoms with vacuum fluctuations of the electromagnetic field leads to both the relaxation of atomic excited states and the renormalization of atomic energy levels. On one hand, the emission of real photons into a single mode of the electromagnetic continuum at the atomic transition frequency results in spontaneous emission. On the other hand, the emission and absorption of virtual photons from all modes of the continuum gives rise to a Lamb shift (a shift in the energy-level separation). In the presence of additional atoms, both real and virtual photons emitted by one atom can be absorbed by another one, giving rise to nontrivial atom-atom interactions. Such interactions are challenging to observe in three dimensions because of the weak electromagnetic fields generated by individual photons and the poor spatial mode matching between the modes of the emitting and absorbing atoms. Nevertheless, signatures of these interactions in the form of super- and subradiant states, which depended on the separation of two trapped ions, were observed (1, 2). Due to the inverse scaling of the interaction strength with interatomic separation, the super- and subradiant lifetimes were observed to differ by only a few percent in these experiments.

Confining both the radiation field and the two-level systems to one dimension overcomes the aforementioned challenges and allows for observing photon-mediated interactions between atoms. This nascent field of physics known as waveguide quantum electrodynamics (QED) is expected to contribute to the development of quantum networks (3), circuits operating on the level of single photons (4, 5), implementations of quantum memories using electromagnetically

induced transparency (6), and the generation of photon-photon interactions (7).

At optical frequencies, realizations of waveguide QED systems have been proposed for quantum dots interacting with surface plasmons (8–12) and for atoms trapped in the near field of a nanofiber (13–16). Superconducting circuits are also a natural choice to investigate the strong interaction of quantum two-level systems with microwave photons in open one-dimensional (1D) transmission lines (17). Near-unity reflectance of weak coherent fields by a single qubit was first observed by Astafiev *et al.* (18). Subsequently, phenomena such as resonance fluorescence, Autler-Townes splitting, electromagnetically induced transparency (19), time-resolved emission dynamics (20), and

the cross-Kerr effect (21) have been explored, and single-photon routers (22) have been realized.

Here, we demonstrate the coupling between two superconducting qubits mediated by microwave photons in a 1D transmission line. In contrast to the 3D case in which the interaction decreases rapidly with increasing separation between the qubits, the interaction in 1D shows behavior at an approximately constant amplitude [see (23) and references therein]. Indeed, the photon-mediated interaction leads to correlated decay of a pair of qubits at a rate $\gamma \propto \cos(2\pi d/\lambda)$ and coherent exchange-type interactions at a frequency $J \propto \sin(2\pi d/\lambda)$. Whereas the interqubit separation d is fixed for a given sample in our experiment, we vary the effective separation between the qubits in terms of their emission wavelength λ . For this purpose, we change the qubit transition frequencies by an appreciable fraction of their maximal values (Fig. 1A), an aspect that is challenging to achieve in most atomic systems.

We have fabricated a sample in which two superconducting transmon qubits (24) are coupled to a 1D coplanar waveguide transmission line at an interqubit separation of $d = 18.6$ nm (Fig. 1A). For both qubits, we have determined the maximum frequency 6.89 and 6.84 GHz of the ground $|g\rangle$ to first excited state $|e\rangle$ transitions and the identical anharmonicity -298 MHz of the first-to-second excited state transition using spectroscopic techniques.

To further characterize the system, we measured the amplitude and phase of a weak drive field coherently scattered from the sample in a detection bandwidth much less than 1 MHz (25).

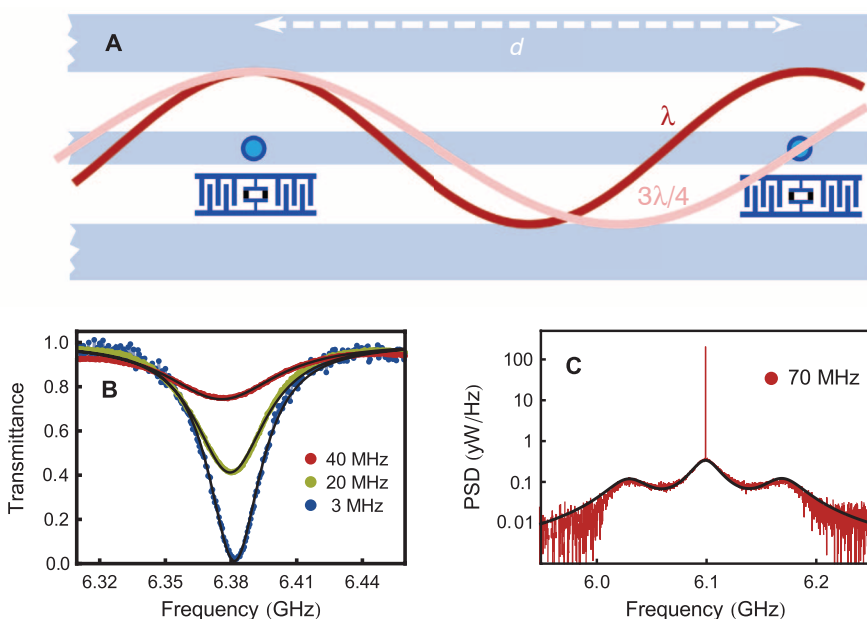


Fig. 1. The experimental system. (A) Schematic of two transmon qubits coupled to an open transmission line at a fixed separation d corresponding to an effective separation of λ or $3\lambda/4$, which is tunable by adjusting the qubit transition frequency. (B) Transmittance spectrum $|t|^2$ of a single qubit measured at the indicated drive rates. (C) Power spectral density (PSD) of the radiation reflected by a single qubit. Red lines are data; black lines denote theory (see text for details). $1 \text{ yW} = 10^{-24} \text{ W}$.

¹Department of Physics, ETH Zurich, CH-8093 Zurich, Switzerland. ²Département de Physique, Université de Sherbrooke, Sherbrooke, Québec J1K 2R1, Canada. ³Institute for Quantum Science and Technology, University of Calgary, Alberta T2N 1N4, Canada.

*Corresponding author. E-mail: arjan@phys.ethz.ch
 †Present address: Australian Research Council Centre for Engineered Quantum Systems, University of Queensland, Brisbane 4072, Australia.

We determined the transmittance $|t|^2$ and reflectance $|r|^2$ (normalized transmitted and reflected power) from the measured transmission and reflection coefficients t and r (25). When either qubit is detuned by many linewidths from the other, we observed no difference in line shape compared to a single qubit. At 6.4 GHz, the minimum transmittance is less than 0.025 for low drive powers (Fig. 1B), indicating strong coupling (25).

From the linewidth, the decay rates of both qubits are determined to be $\gamma_1/2\pi \approx 26 \pm 1$ MHz at 6.4 GHz, and 13 ± 1 MHz at 4.8 GHz, consistent with expectations for an ohmic environment (18). When the power of the incident drive field is increased, the qubit transition saturates (26), and transmittance increases to unity for large drive powers (Fig. 1B).

When the two qubits are tuned into resonance, such that a photon emitted by one of the qubits may be absorbed by the other, we expect correlated effects to become apparent. For both qubits tuned to either 6.4 or 4.8 GHz, corresponding to an effective qubit separation d of λ or $3\lambda/4$, respectively, we tune the qubits through resonance and plot $|t|^2$ and $|r|^2$ versus frequency (Fig. 2). When the qubits are detuned from each other by much more than the range displayed in Fig. 2, they each display a pronounced well-resolved maximum in $|r|^2$, similar to data obtained for a single qubit. When the two qubits are in resonance with

each other for $d \sim \lambda$, only a single resonance is observed, with $|r|^2$ reaching unity at mutual resonance and $|t|^2$ going to zero (Fig. 2B).

These observations can be understood by considering photon-mediated interactions between the two qubits (23). When $d \sim \lambda$, the exchange interaction $J = 0$ and the correlated decay rate takes its maximal value $\gamma = \gamma_1$. This type of decay leads to subradiant, $|D\rangle = (|ge\rangle - |eg\rangle)/\sqrt{2}$, and superradiant, $|B\rangle = (|ge\rangle + |eg\rangle)/\sqrt{2}$, states (1). When the qubits are separated by λ , they are driven with the same phase by a single drive tone. Therefore, the symmetric state $|B\rangle$, which has the same symmetry as the drive at the qubits, can be excited from the ground state $|gg\rangle$. Thus, this state is bright. In contrast, the matrix element for the antisymmetric state $|D\rangle$, which has opposite symmetry with respect to both the drive field and the resonant vacuum fluctuations that cause relaxation, is zero. Because the latter is dark, the two-qubit system essentially behaves as a single two-level system with ground state $|gg\rangle$ and excited state $|B\rangle$ at low drive powers with the superradiant decay rate $\Gamma_B = 2\gamma_1$ (23). The two-qubit results (Fig. 2B) are qualitatively similar to those of a single qubit (Fig. 1B), but with a linewidth $\Gamma_B/2\pi \sim 52 \pm 1$ MHz, which is twice as large as the one extracted for a single qubit. This is a clear signature of superradiance.

The situation is more subtle when the qubits are separated by $d \sim 3\lambda/4$ or any odd multiple of

$\lambda/4$. Then one of the qubits is at a node of the driving field, whereas the other is at an antinode (Fig. 1A). In this case, the above argument leading to the creation of bright and dark states does not apply, and correlated decay is absent with $\gamma = 0$. Instead, the coherent exchange interaction between qubits mediated by virtual photons takes its maximal value $J = \gamma_1/2$ (27).

The expected signature of this coherent exchange interaction is an anticrossing of the qubit energy levels similar to the one observed for two qubits coupled to a resonator in a circuit QED system (28, 29). As the expected splitting $2J = \gamma_1$ can be only as large as the peak width γ_1 , this signature is not apparent in the elastic scattering data. The doublet observed in reflection in Fig. 2D is a consequence of dressing of the two-qubit system by the input field rather than a signature of exchange interaction (25). The quantitative analysis presented in (23) (solid black lines) agrees with the data (colored lines) over the full range of frequencies shown in Fig. 2.

To further characterize photon-mediated atom-atom interactions, the full spectrum of the elastically and inelastically scattered radiation, including the Rayleigh scattered and resonance fluorescence contributions, has been recorded in both reflection and transmission (25). In a reference measurement of the resonance fluorescence spectrum of a single qubit, we observe the standard Mollow triplet (30), including a δ -like peak due to elastically (Rayleigh) scattered radiation (Fig. 1C). The Mollow sidebands appear at a detuning

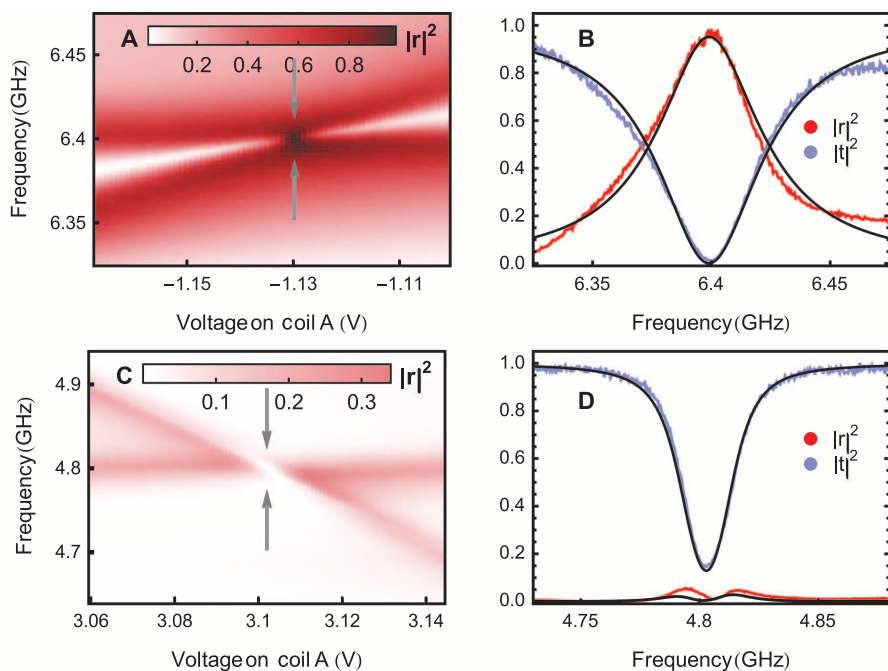


Fig. 2. Elastically scattered radiation. Reflectance spectra $|r|^2$ of the two-qubit system [(A) and (B)] at $d \sim \lambda$ recorded with a drive rate of 7.5 MHz and [(C) and (D)] at $d \sim 3\lambda/4$ with rate 8.7 MHz (red data sets). In (B) and (D), the transmittance $|t|^2$ is also shown (blue data sets). In (A) and (C), the frequency of one qubit is tuned by applying the indicated voltages to millimeter-size coils integrated in the sample mount, whereas the other qubit is kept at a fixed frequency. Close to resonance, interference effects cause the qubit peaks to become asymmetric. (B) and (D) show spectra at bias points indicated by arrows in (A) and (C), respectively. Colored lines are data; black lines denote theory (see text for details).

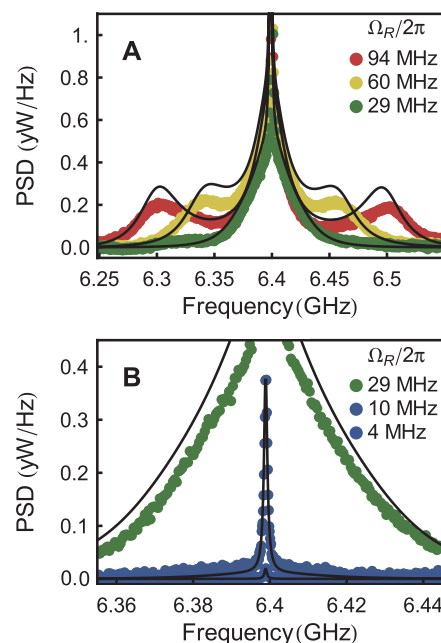


Fig. 3. Super- and subradiance. (A and B) Power spectral density measured in reflection for two qubits in resonance at $d \sim \lambda$ at the indicated Rabi drive rates Ω_R . Solid lines are numerical calculations (23) using the parameters specified in the supplementary materials (25).

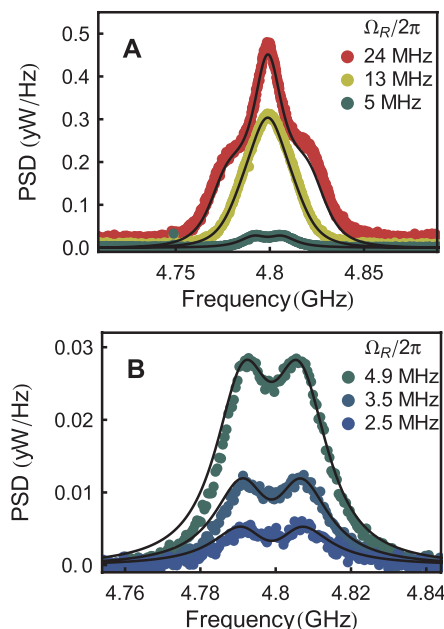


Fig. 4. Exchange interaction. (A and B) Power spectral density measured in transmission for two qubits in resonance at $d \sim 3\lambda/4$ at the indicated Rabi drive rates Ω_R . Solid lines are as in Fig. 3.

from the center peak corresponding to the Rabi frequency induced by the drive.

When both qubits are tuned to 6.4 GHz corresponding to $d \sim \lambda$, we observe a Mollow triplet-like spectrum with a narrow resonance superimposed at its center frequency (Fig. 3). The narrow resonance becomes more discernible as the drive power is decreased (Fig. 3B). Here and below, the Rayleigh scattered contribution was removed from the data for clarity. These two distinct features, the Mollow triplet and narrow resonance, are due to the formation of super- and subradiant states, respectively.

The effective two-level system $\{|gg\rangle, |B\rangle\}$ is strongly dressed by the drive field, resulting in a Mollow triplet. The width ~ 52 MHz of the main peak, obtained by fitting to numerical calculations (black lines in Fig. 3), is consistent with the value of Γ_B extracted above. Ideally, the dark state $|D\rangle$ is neither excited by the drive nor does it decay into $|gg\rangle$ due to selection rules. In practice, however, it is weakly populated due to qubit dephasing, nonradiative decay from the state $|ee\rangle$, and unequal single-qubit relaxation rates (23). As a result, the dark state $|D\rangle$ appears as a narrow resonance superimposed on the bright-state Mollow triplet. Its linewidth, when compared to numerical results, is approximately $\Gamma_D/2\pi \sim 0.4 \pm 0.2$ MHz. We obtain adequate quantitative agreement between the measured spectra and theory (see lines in Fig. 3) and find the ratio between super- and subradiant lifetimes to be as high as $\Gamma_B/\Gamma_D \geq 100$.

When both qubits are tuned to 4.8 GHz, corresponding to $d = 3\lambda/4$, the resonance fluorescence spectra at high powers ($\Omega_R/2\pi \geq 15$ MHz, where Ω_R is the Rabi drive rate) also display the

expected Mollow triplet features (Fig. 4A). At drive powers much lower than the relaxation rate $\Omega_R/2\pi \leq 5$ MHz, the fluorescence spectrum displays a double-peak structure split by ~ 15 MHz (see Fig. 4B). This observation is a clear signature of the effective exchange interaction J between the two qubits mediated by virtual photons. The observed splitting is slightly larger than the expected value $2J/2\pi = \gamma_1/2\pi \approx 13$ MHz, which is consistent with theory predicting the splitting to be larger than $2J$ in transmission and smaller in reflection (23).

Our results present compelling evidence of strong interaction effects between two superconducting qubits separated by as much as a full wavelength $\lambda \sim 18.6$ mm in an open 1D environment. The observation of these effects presents opportunities to explore decoherence-free subspaces and entanglement over long distances in open environments and could lead to exciting applications in quantum communication technology.

References and Notes

- R. G. DeVoe, R. G. Brewer, *Phys. Rev. Lett.* **76**, 2049–2052 (1996).
- J. Eschner, C. Raab, F. Schmidt-Kaler, R. Blatt, *Nature* **413**, 495–498 (2001).
- H. J. Kimble, *Nature* **453**, 1023–1030 (2008).
- D. E. Chang, A. S. Sørensen, E. A. Demler, M. D. Lukin, *Nat. Phys.* **3**, 807–812 (2007).
- J. Hwang *et al.*, *Nature* **460**, 76–80 (2009).
- P. M. Leung, B. C. Sanders, *Phys. Rev. Lett.* **109**, 253603 (2012).
- H. Zheng, D. J. Gauthier, H. U. Baranger, *Phys. Rev. A* **85**, 043832 (2012).
- D. E. Chang, A. S. Sørensen, P. R. Hemmer, M. D. Lukin, *Phys. Rev. Lett.* **97**, 053002 (2006).
- D. E. Chang, A. S. Sørensen, P. R. Hemmer, M. D. Lukin, *Phys. Rev. B* **76**, 035420 (2007).
- A. V. Akimov *et al.*, *Nature* **450**, 402–406 (2007).
- D. Martín-Cano, L. Martín-Moreno, F. J. García-Vidal, E. Moreno, *Nano Lett.* **10**, 3129–3134 (2010).
- A. Gonzalez-Tudela *et al.*, *Phys. Rev. Lett.* **106**, 020501 (2011).

- K. P. Nayak *et al.*, *Opt. Express* **15**, 5431–5438 (2007).
- E. Vetsch *et al.*, *Phys. Rev. Lett.* **104**, 203603 (2010).
- D. E. Chang, L. Jiang, A. V. Gorshkov, H. J. Kimble, *New J. Phys.* **14**, 063003 (2012).
- A. Goban *et al.*, *Phys. Rev. Lett.* **109**, 033603 (2012).
- J.-T. Shen, S. Fan, *Phys. Rev. Lett.* **95**, 213001 (2005).
- O. Astafiev *et al.*, *Science* **327**, 840–843 (2010).
- A. A. Abdumalikov Jr. *et al.*, *Phys. Rev. Lett.* **104**, 193601 (2010).
- A. A. Abdumalikov Jr., O. V. Astafiev, Y. A. Pashkin, Y. Nakamura, J. S. Tsai, *Phys. Rev. Lett.* **107**, 043604 (2011).
- I.-C. Hoi *et al.*, *Phys. Rev. Lett.* **111**, 053601 (2013).
- I.-C. Hoi *et al.*, *Phys. Rev. Lett.* **107**, 073601 (2011).
- K. Lalumière *et al.*, *Phys. Rev. A* **88**, 043806 (2013).
- J. Koch *et al.*, *Phys. Rev. A* **76**, 042319 (2007).
- Materials and methods are available as supplementary materials on Science Online.
- I.-C. Hoi *et al.*, *Phys. Rev. Lett.* **108**, 263601 (2012).
- Whereas correlated decay mediated by the exchange of real photons is absent when one of the qubits is at an antinode of the field, the exchange of virtual photons is still possible, as it is caused by virtual photons at all frequencies except the qubit transition frequency.
- J. Majer *et al.*, *Nature* **449**, 443–447 (2007).
- S. Filipp *et al.*, *Phys. Rev. A* **83**, 063827 (2011).
- B. R. Mollow, *Phys. Rev.* **188**, 1969–1975 (1969).

Acknowledgments: We acknowledge financial support by Canadian Institute for Advanced Research, Natural Sciences and Engineering Research Council of Canada, Alberta Innovates Technology Futures, and ETH Zurich, and we thank Calcul Québec and Compute Canada for computational resources. Furthermore, we thank L. Steffen for sample fabrication, C. Lang and Y. Salathé for realizing the firmware for measuring power spectral densities using field-programmable gate array-based electronics, M. Boissonneault for help with numerical simulations, and V. Sandoghdar for initial discussions motivating this work.

Supplementary Materials

www.sciencemag.org/content/342/6165/1494/suppl/DC1
Materials and Methods
References

6 August 2013; accepted 16 October 2013

Published online 14 November 2013;

10.1126/science.1244324

Relaxation Mechanism of the Hydrated Electron

Madeline H. Elkins,¹ Holly L. Williams,¹ Alexander T. Shreve,² Daniel M. Neumark^{1,3*}

The relaxation dynamics of the photoexcited hydrated electron have been subject to conflicting interpretations. Here, we report time-resolved photoelectron spectra of hydrated electrons in a liquid microjet with the aim of clarifying ambiguities from previous experiments. A sequence of three ultrashort laser pulses (~ 100 femtosecond duration) successively created hydrated electrons by charge-transfer-to-solvent excitation of dissolved anions, electronically excited these electrons via the $s \rightarrow p$ transition, and then ejected them into vacuum. Two distinct transient signals were observed. One was assigned to the initially excited p -state with a lifetime of ~ 75 femtoseconds, and the other, with a lifetime of ~ 400 femtoseconds, was attributed to s -state electrons just after internal conversion in a nonequilibrated solvent environment. These assignments support the nonadiabatic relaxation model.

The hydrated electron e_{aq}^- is a species of fundamental interest in the chemistry of water. It has been implicated in phenomena ranging from aerosol nucleation to radiation

damage in DNA (I). As the simplest quantum solute, with only a single electronic degree of freedom, it has been the focus of many experimental and theoretical studies over the years (2–4). None-